Dual control of caveolar membrane traffic by microtubules and the actin cytoskeleton

Dorothy I. Mundy[1,*], Thomas Machleidt[1], Yun-shu Ying[1], Richard G. W. Anderson[1] and George S. Bloom[2]

[1]Department of Cell Biology, University of Texas Southwestern Medical Center, Dallas, Texas 75390-9039, USA
[2]Departments of Biology and Cell Biology, University of Virginia, Charlottesville, Virginia 22903, USA
*Author for correspondence (e-mail: dorothy.mundy@utsouthwestern.edu

Accepted 21 August 2002
Journal of Cell Science 115, 4327-4339 © 2002 The Company of Biologists Ltd
doi:10.1242/jcs.00117

Summary

Live cell, time-lapse microscopy was used to study trafficking of caveolin-1-GFP in stably expressing CHO cells. Multiple cytological and biochemical tests verified that caveolin-1-GFP was a reliable marker for endogenous caveolin-1. At steady state, most caveolin-1-GFP was either at the cell surface associated with invaginated caveolae or near the centrosome in caveosomes. Live cell fluorescence imaging indicated that while much of the caveolin-1-GFP in caveolae at the cell surface was relatively sessile, numerous, highly motile caveolin-1-GFP-positive vesicles were present within the cell interior. These vesicles moved at speeds ranging from 0.3-2 μm/second and movement was abolished when microtubules were depolymerized with nocodazole. In the absence of microtubules, cell surface invaginated caveolae increased more than twofold and they became organized into linear arrays. Complete depolymerization of the actin cytoskeleton with latrunculin A, by contrast, triggered rapid and massive movements of caveolin-positive structures towards the centrosomal region of the cell. The caveolar membrane system of CHO cells therefore appears to be comprised of three caveolin-1-containing compartments. These include caveolae that are confined to the cell surface by cortical actin filaments, the peri-centrosomal caveosomes and caveolar vesicles, which we call 'cavicles', that move constitutively and bi-directionally along microtubules between the cell surface and caveosomes. The behavior of cavicles suggests that they function as transport intermediates between caveolae and caveosomes.

Movies available online

Key words: Caveolin, Recycling endosome, Caveolae, Caveosome

Introduction

A detailed understanding of how microtubules are involved in membrane trafficking is rapidly emerging, but the role of actin filaments in this process remains relatively unknown. Microtubules serve as tracks for long range, rapid movements of transport intermediates between donor and acceptor compartments in the secretory and the endocytic pathways (Bloom and Goldstein, 1998). In addition, microtubules control the movement of organelles such as mitochondria and peroxisomes and the steady state distribution of the ER, the Golgi apparatus, endosomes and lysosomes. Actin filaments also appear to be involved in organelle and vesicle movements particularly along axons (Kuznetsov et al., 1992) and in microvilli (Fath and Burgess, 1993) but in general these movements occur both within a shorter range and have slower velocities than microtubule based movements.

Interestingly, there are several recent studies that show the movements of some organelles and vesicles are controlled by both microtubules and actin filaments. These include movement of phagosomes in macrophages (Al-Haddad et al., 2001), of lysosomes in hepatoma cells (Cordonnier et al., 2001), of mitochondria and other vesicles in neurons (Bridgman, 1999; Morris and Hollenbeck, 1995) and of pigment granules within the extensions of pigment producing cells (Rodionov et al., 1998; Rogers and Gelfand, 1998; Wu et al., 1998). The distribution of pigment granules in melanocytes provides a striking example of this coordinate control by both of these cytoskeletal arrays. Long distance, bi-directional movements of the granules occur along radially arranged microtubules, and require microtubule motor proteins of the kinesin and dynein families. In contrast, more spatially restricted movements occur along actin filaments and make use of the actin motor myosin Va (Rogers and Gelfand, 2000). Myosin Va also appears to be required to tether pigment granules to actin filaments located in the cell periphery and this is the mechanism responsible for determining the steady state distribution of the granules (Wu et al., 1998). Both microtubule and actin filaments may also play roles in the intracellular movement of endocytic membrane generated from clathrin coated pits (Apodaca, 2001). Actin seems to be important for events that take place during the budding process (Kamal et al., 1998; Lamaze et al., 1997) while microtubules appear to be responsible for the movement of newly budded endocytic vesicles to different sites within the cell (Kamal et al., 1998; Valetti et al., 1999). By contrast, little is known about how the cytoskeleton controls the dynamics of caveolae and the transport intermediates that might communicate with them.

Caveolae, or plasmalemmal vesicles, were originally described as flask-shaped, plasma membrane invaginations found in gall bladder epithelial and endothelial cells (Palade, 1953; Yamada, 1955) but are now known to be present in a broad variety of cell types (Anderson, 1998). Numerous

morphological studies have documented that caveolae mediate the movement of molecules across endothelial cells (Simionescu, 1983). Transcytosis appears to involve membrane invagination, vesicle budding and movement of vesicles filled with cargo to the opposite side of the cell. The principle method used to identify caveolae in these studies is their shape. A morphologic membrane signature works well in thin endothelial cells where vesicles travel only short distances to traverse the cell. In most cells, however, caveolae-derived transport intermediates rapidly mix with structures of similar morphology originating from other membrane compartments. As a consequence, it is very difficult to track the movement of caveolae-derived membranes in most cells.

The standard method for mapping the traffic of intracellular membranes is to follow the movement of a visible marker for that membrane. A well-accepted marker for caveolae in fibroblasts is caveolin-1 (Rothberg et al., 1992). This integral membrane protein is a component of the cytoplasmic, filamentous coat that decorates the cytoplasmic surface of fibroblast and endothelial cell caveolae. Attachment of green fluorescence protein (GFP) to the C-terminal end of the molecule does not appear to interfere with its localization to caveolae (Pelkmans et al., 2001). Previous studies suggest that caveolin-1-GFP collects at sites of cell-cell contact (Volonte et al., 1999) and along the cleavage furrow during cytokinesis (Kogo and Fujimoto, 2000). Caveolin-1-GFP has also been used to show that SV-40 virus is internalized by caveolae and delivered to a unique endocytic compartment called a caveosome (Pelkmans et al., 2001).

Here we describe caveolin-1 dynamics in CHO cells stably transfected with caveolin-1-GFP. We observed the fluorescent fusion protein in caveolae and the caveosome, and in constitutively motile vesicles and tubules that evidently serve as transport intermediates between them. Furthermore, because perturbation of either microtubules or actin filaments caused rapid and profound changes in the dynamics and localization of caveolin-1-GFP, we conclude that these two structurally distinct components of the cytoskeleton act coordinately to regulate trafficking of the caveolar membrane system.

Materials and Methods

Construction of caveolin-1-GFP and generation of stable caveolin-1-GFP-expressing cell lines

GFP was attached to the C-terminal end of caveolin-1. *Hin*dIII restriction sites were added to both 5′ and 3′ ends of the human caveolin-1 cDNA by PCR using the Expand High Fidelity PCR system (Roche Molecular Biochemicals, Indianapolis, IN). The PCR product was digested with *Hin*dIII and inserted into the *Hin*dIII site of the EGFP-N1 eukaryotic expression vector (Clontech, Palo Alto, CA). The proper orientation and sequence of caveolin-1-GFP were verified by sequencing. The polybrene method (Brewer, 1994) was used to transfect CHO K1 cells with the caveolin-1-GFP construct. Transfected cells were selected by growing in 0.8 mg/ml G418 (Invitrogen, Carlsbad, CA) for 14 days. Individual clones were isolated and screened for expression of the caveolin-1-GFP by fluorescence microscopy, expanded and then frozen for future use. The transfected CHO cells used in each experiment were maintained in DME (Invitrogen, Carlsbad, CA) supplemented with 10% FCS plus and 40 μg/ml proline in a humidified CO_2 (5%) incubator at 37°C. New batches of cells were established from frozen stocks every 10-12 weeks. Normal human fibroblasts were grown as previously described (Goldstein et al., 1983).

Live cell imaging

For live cell recordings, cells were sub-cultured at least 2 days before each experiment into 35 mm dishes which had been modified with a hole in the bottom to which a #1 thickness glass coverslip was glued (Mat Tek Corp, Ashland, MA). The dishes were placed in a humidified Plexiglas chamber and maintained at 37°C and 5% CO_2 throughout each experiment. We did not see any effect of either the number of days in culture or cell density on caveolin-1-GFP movement. Cells were imaged using a Leica TCS-SP laser scanning confocal microscope with a 100×, 1.4 NA, plan-apochromatic lens using a computer controlled 488 nm argon laser to excite GFP or a 568 nm krypton laser to excite Alexa red dyes. Signals were collected at 1.6 second intervals using a photomultiplier tube, digitized (512×512 pixels) and converted into images using Leica TCS software. FRAP (fluorescence recovery after photobleach) was performed by exposing 3-10 bleach spots in areas of interest and bleaching with the 488 laser line at full power for 2 seconds. The Leica TCS software was used to quantify fluorescent intensities in photobleached regions, which were corrected for overall bleaching by comparison with areas that were not exposed to the full power of the laser.

Immunofluorescence and immunogold electron microscopy

Cells plated onto coverslips in 12-well dishes were fixed either with 4% paraformaldehyde (PFA) in PBS at room temperature or with methanol at –20°C. Cells fixed with PFA were permeabilized with 0.2% TX-100. Non-specific binding sites were blocked by incubating coverslips for 30 minutes in PBS containing 1% fish skin gelatin (Sigma, St Louis, MO). Fixed cells were incubated with primary antibodies diluted in PBS containing 1% fish skin gelatin for 30 minutes, washed with PBS several times and then incubated with the appropriate secondary antibodies conjugated to the specified Alexa dyes (Molecular Probes, Eugene, OR) for 30 minutes before mounting with Aqua Poly/mount Polysciences). Images were collected using the Leica TCS-SP laser scanning confocal microscope and processed using Adobe Photoshop. Images usually consisted of from 10-16 optical slices in order to span the entire depth of the cell. Mouse anti-transferrin receptor (Zymed, San Francisco, CA) was used to label recycling endosomes in CHO cells. Rabbit anti-mannosidase II was kindly provided by Kelly Moreman. For electron microscopy (EM) analysis, cells were processed for indirect immunogold detection of either GFP or caveolin-1 and quantified as previously described (Smart et al., 1994).

Isolation of Triton-X-100-insoluble membranes, velocity sedimentation and immunoblotting

Triton-X-100-insoluble membranes were isolated as previously described (Liu and Anderson, 1995) with the following changes. Briefly, two 100 mm dishes of confluent CHO cells stably expressing caveolin-1-GFP were washed twice with ice cold buffer A (12.5 mM MES, 75 mM NaCl, pH 6.5). The cells were then scraped from the dish and solubilized in 1 ml of buffer B (1% Triton X-100 in buffer A containing 10 μM leupeptin, 500 μM benzamindine, 10 μg/ml soybean trypsin inhibitor, 1 μg/ml pepstatin A, 200 μg/ml phenylmethylsulfonyl fluoride and 1 mM EDTA) and incubated on ice for 20 minutes. The sample was then homogenized with a dounce homogenizer 20 times, mixed with 1 ml of 2.5 M sucrose in buffer A and loaded on the bottom of a 12-ml ultracentrifuge tube. The sample was overlaid with 8 mls of a 10-30% sucrose gradient in buffer A and centrifuged at 29,000 ***g*** for 21 hours at 4°C in a SW41 rotor. Equal fractions (700 μl) were collected and the protein was precipitated by adding TCA and deoxycholate (final concentrations 7% and 0.015%, respectively) from concentrated stock solutions. The pellets were washed once with acetone, solubilized in sample buffer (Laemmli, 1970) and separated by SDS-PAGE. Proteins were transferred to PVDF membranes at 20-30 volts overnight in transfer buffer (25 mM

Tris, 192 mM glycine). Membranes were processed for immunoblotting by first incubating for 30 minutes in PBS containing 5% dried milk powder and 0.05% Tween 20 (blocking buffer) followed by incubating with primary antibody diluted in the same buffer for 1 hour. The membranes were washed 3-5 times in PBS/0.05% Tween 20 and then incubated with a horseradish peroxidase (HRP) conjugated secondary antibody (Biorad, Hercules, CA) in blocking buffer for 1 hour. After extensive washing, antibodies were detected using chemiluminescence (Amersham Biosciences, Piscataway, NJ**)**. Velocity sedimentation analysis of caveolin-1-GFP was performed as previously described (Machleidt et al., 2000).

Palmitate labeling

Cells were plated in 60 mm dishes and incubated in the presence of 500 μCi of [^{3}H]-palmitate (NEN, Boston, MA) for 2.5 hours at 37°C. Each dish was washed 2 times with PBS and scraped on ice into 1 ml buffer C (25 mM Tris-HCl.pH7.5, 5 mM EDTA, 150 mM NaCl, 1% Triton X-100 and 60 mM n-octyl-β-D-glucopyranoside) and solubilized on ice for 1 hour. The samples were cleared by centrifugation at high speed in an Eppendorf microcentrifuge for 10 minutes. Caveolin and caveolin-1-GFP were immunoprecipitated by incubating overnight with 16 μl of a polyclonal anti-caveolin-1 antibody (Transduction Laboratories, Lexington, KY) and the immune complexes collected by adding 50 μl of protein G-agarose (Sigma, St Louis, MO) for 1 hour. The precipitates were washed 3 times with buffer C, solubilized in sample buffer containing 10 mM DTT by boiling and separated by SDS-PAGE on a 5-20% gradient gel. Gels were treated with Amplify (Amersham Biosciences, Piscataway, NJ) and dried for autoradiography. Films were developed after 7 days.

Results

Caveolin-1-GFP is a reliable marker for endogenous caveolin-1

To examine the intracellular trafficking of caveolin-1, we fused the C-terminal end of wild-type caveolin-1 to green fluorescence protein (GFP) and established a stable cell line expressing this protein. Several criteria were used to establish that this chimeric protein behaved like endogenous caveolin-1. One of the properties of caveolin-1 is that it is resistant to extraction in cold Triton X-100. Enriched fractions of detergent insoluble membranes were isolated from cells, fractionated on sucrose gradients and analyzed by immunoblotting with anti-caveolin-1 (Fig. 1A). The low-density membranes migrated towards the top of the gradient (fractions 6-12), as judged by the presence of caveolin-1 (Fig. 1A). The distribution of caveolin-1-GFP was indistinguishable from that of endogenous caveolin-1, indicating that the chimeric protein was also associated with detergent insoluble caveolae (Cav-GFP, Fig. 1A). Comparison of the immunoreactive signals for caveolin-1-GFP and caveolin-1 demonstrated that the fluorescent fusion protein was expressed at a low level compared to caveolin-1. Quantification of immunoblots from this and similar experiments indicate that the molar ratio of caveolin-1-GFP to endogenous caveolin-1 ranged from 0.2 to 0.3 in the stably transfected CHO cells. Immunofluorescence microscopy showed that the expression levels were relatively constant from cell to cell and non-expressing cells were very rare. Caveolin-1-GFP was also palmitoylated (Dietzen et al., 1995), indicating that the transfected protein trafficked through the same compartments as the endogenous protein (Fig. 1B). The attachment of GFP to caveolin-1 also did not alter the ability of caveolin-1 to oligomerize, another important property of native caveolin-1 (Monier et al., 1996). This was indicated by

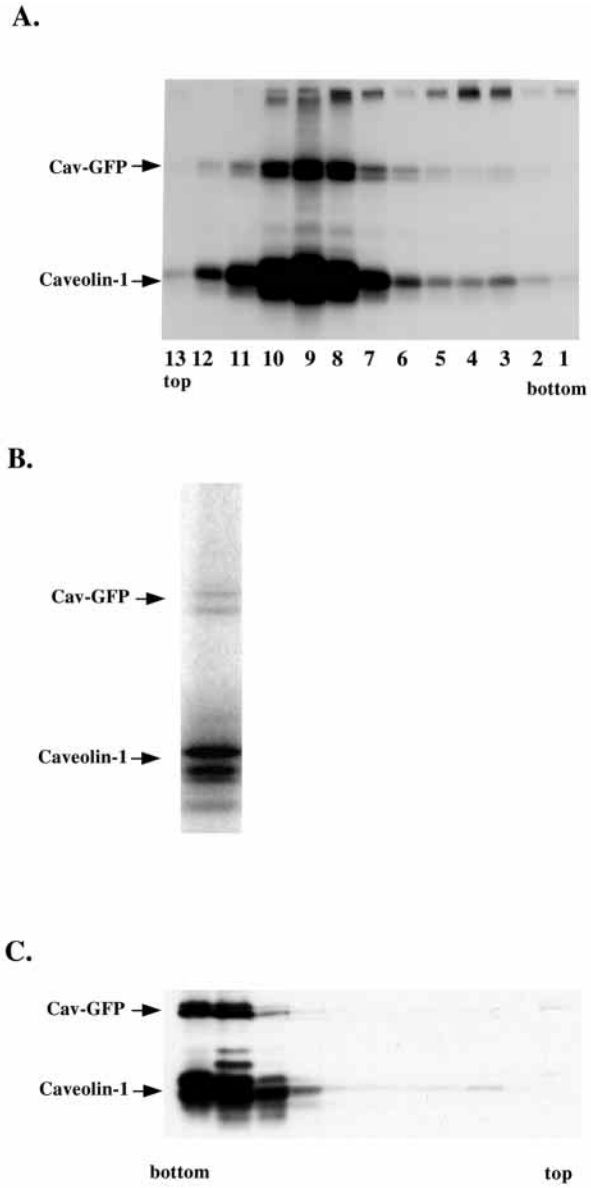

Fig. 1. Caveolin-1-GFP behaves like endogenous caveolin-1. CHO cells stably transfected with caveolin-1-GFP were grown for 2 days until confluent. (A) Triton X-100-insoluble caveolae were separated from soluble membranes on sucrose gradients and immunoblotted with anti-caveolin-1. Caveolin-1-GFP (Cav-GFP) co-fractionated with endogenous caveolin-1 (Caveolin-1). The intensity of the bands for the two proteins indicates that caveolin-1-GFP constitutes a minor amount of the total caveolin-1 pool. (B) Cells were incubated for 2.5 hours in the presence of ^{3}H-palmitate to label acylated proteins. Caveolin-1 was immunoprecipitated, separated by PAGE and processed for autoradiography. Both the endogenous protein (caveolin-1) and the caveolin-1-GFP (cav-GFP) were covalently labeled with ^{3}H-palmitate. (C) Caveolin was extracted from cells using a combination of Triton X-100 and deoxycholate to solubilize the caveolar membranes and then analyzed by velocity gradient sedimentation. Both the endogenous caveolin (caveolin-1) and caveolin-1-GFP (cav-GFP) form oligomers that migrate to the bottom of the gradient.

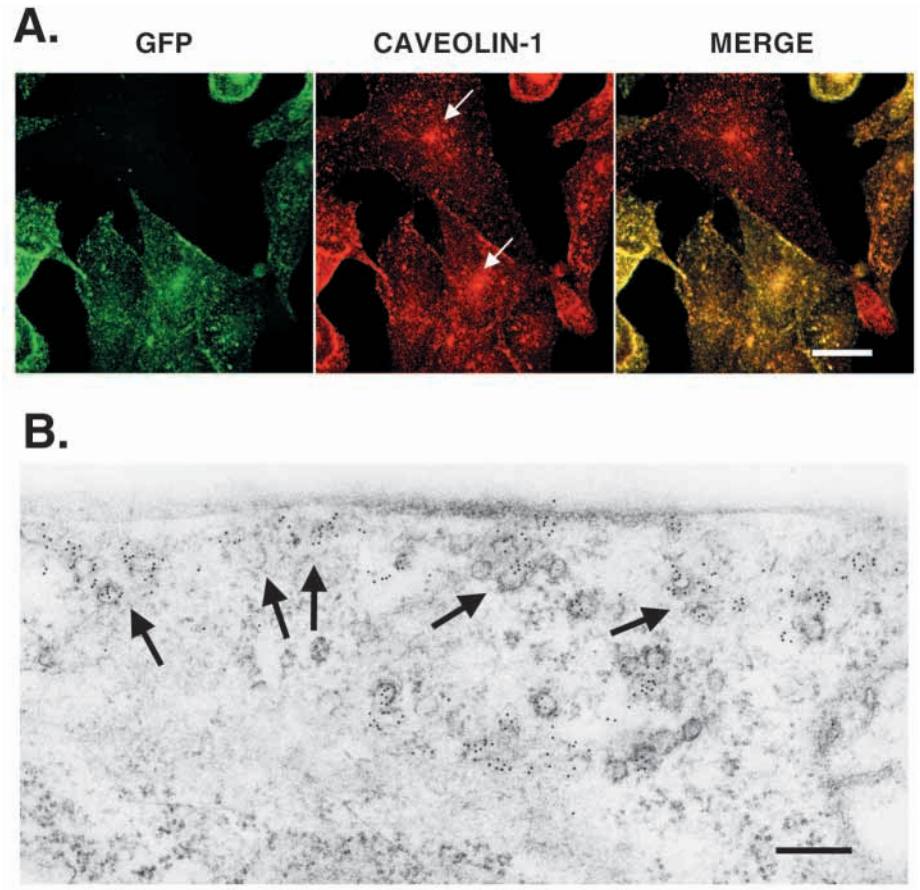

Fig. 2. Caveolin-1-GFP is located in caveolae. (A) A mixed culture of parental CHO cells and CHO cells stably expressing the caveolin-1-GFP were plated on coverslips and grown for 2 days before they were fixed in methanol and labeled with anti-caveolin-1 followed by an Alexa-568-labeled goat anti-rabbit IgG. The green channel (GFP) shows only those cells that express caveolin-1-GFP, while the red channel shows anti-caveolin-1 staining. The anti-caveolin-1 antibody detects both endogenous caveolin-1 and caveolin-1-GFP. The merged image shows nearly perfect overlap indicating that all of the GFP signal is from caveolin-1-GFP and not from GFP that has been cleaved from the caveolin. The addition of a GFP moiety has not affected the distribution of caveolin (compare the caveolin distribution in the non-expressing cell at the top with one that is expressing the GFP construct below it). (B) Cells were grown for 2 days in 6-well tissue culture dishes and incubated for 1.75 hours in the presence of 10 μM nocodazole, which was used to enhance our ability to recognize caveolae at the cell surface of these cells. The samples were then fixed and processed for immunogold localization of GFP. Bars, 20 μm (A); 0.25 μm (B).

co-fractionation of the fusion protein with caveolin-1 containing high density complexes on sucrose gradients of membranes solubilized with a mixture of Triton-X-100 and deoxycholate (Fig. 1C). Immunofluorescence microscopy (Fig. 2A) and immunogold EM (Fig. 2B) were also used to determine the distribution of caveolin-1-GFP in these cells. The caveolin-1-GFP fluorescence closely matched the distribution of the anti-caveolin staining, indicating that the GFP probe was not mislocalized. Moreover, the caveolin-1 staining patterns in transfected and non-transfected cells were indistinguishable (Fig. 2A). Finally, the gold label was principally associated with vesicles and cell surface invaginations (arrows) that had the characteristic morphology of caveolae. Taken together, these data establish that caveolin-1-GFP is a valid fluorescent indicator of native caveolin-1 and can be used to study caveolin-1 traffic in live cells.

Caveosomes are clustered near the microtubule organizing center in close proximity to recycling endosomes in CHO cells

Conventional immunofluorescence of normal human fibroblasts has shown that caveolin-1 is frequently concentrated in patches at the edge of the cell and in linear arrays over the cell surface (Rothberg et al., 1992). Confocal imaging of caveolin-1-GFP in CHO cells showed a similar pattern (Fig. 2A). In addition to the typical surface staining of caveolin however, confocal optical sections taken through the cell showed that there were numerous scattered puncta of caveolin-1 throughout the cytoplasm and a prominent accumulation of caveolin positive membranes at the center of the cell (Fig. 2A, arrows). This peri-nuclear structure did not co-localize with the Golgi apparatus markers, mannosidase II (Fig. 3D-F) or GM130 **(**data not shown). Instead, it accumulated near the microtubule-organizing center (MTOC), which was visualized by anti-tubulin staining (Fig. 3A-C). The recycling endosome is also located near the MTOC in CHO cells. To compare the distribution of the caveolin-1-GFP compartment with recycling endosomes, cells were stained with anti-transferrin receptor antibody. Fig. 3G-I shows that caveolin-1-GFP and the transferrin receptor were highly concentrated within the same peri-centrosomal region. Caveolin-1-GFP generally covered a broader area than the transferrin receptor and at high magnification appeared to be largely distinct, although tightly intertwined with the compartment stained by the transferrin receptor antibody. Caveolin-1 positive membranes and recycling endosomes, therefore, share an overlapping distribution in these cells.

Motility of caveolin-1-GFP

The trafficking of caveolin-1-GFP was observed in living cells by confocal, time-lapse microscopy and was found to be remarkably dynamic. At least three different types of movement were seen. Many of the caveolin-1-GFP patches at the cell surface were relatively immobile (yellow arrows, Fig. 4A), exhibiting only localized tethered movements. Occasionally a patch of caveolin-1-GFP appeared to move away from the cell

surface, as if it were budding from the membrane, but these events were rare and difficult to capture. Since EM showed that cell surface caveolin-1-GFP was primarily associated with caveolae membranes (Fig. 2), we conclude that a substantial proportion of the caveolae in these cells are sessile. The possibility remains, however, that these seemingly immotile caveolae internalize and recycle locally without being detected by time lapse fluorescence microscopy (Anderson et al., 1992).

In addition to being localized at the cell surface, caveolin-1-GFP was observed in vesicle-like structures that commonly exhibited rapid movement along curvilinear paths within the cytoplasm. These movements were most visible near the lower surface of the cells just below the nucleus where the surface area is large. The velocities and distances traveled by these caveolar vesicles, or 'cavicles', were quite variable. Eighteen recordings in 15 different cells, were used to determine the apparent instantaneous velocities of individual cavicles and these ranged from 0.3-2.0 μm/seconds with uninterrupted movements that ranged from 2-16 μm. These rapid movements occurred in all directions, and frequently were interrupted by short pauses. A dramatic example of one of these long-range movements is shown in Fig. 4A (separation of white arrows). Many other examples are shown in the accompanying movies (http://jcs.biologists.org/supplemental) (Fig. 4C).

In cells expressing caveolin-1-GFP, we also routinely saw thin tubules decorated with caveolin-1-GFP (yellow arrows, Fig. 4B). These tubules were very dynamic and formed networks that would break, reform and undergo rippling movements (Fig. 4B; see also movies online). The tubules did not appear to be induced by overexpression of caveolin-1-GFP because they were observed in cells expressing both high and low levels of the fusion protein. These structures were not evident in conventionally fixed, untreated cells, however, implying that the tubules do not survive chemical fixation. We do not know the origin of these tubules, but they were present both at the cell periphery and in association with caveolin-1-GFP positive membranes that accumulate near the centrosome in CHO cells.

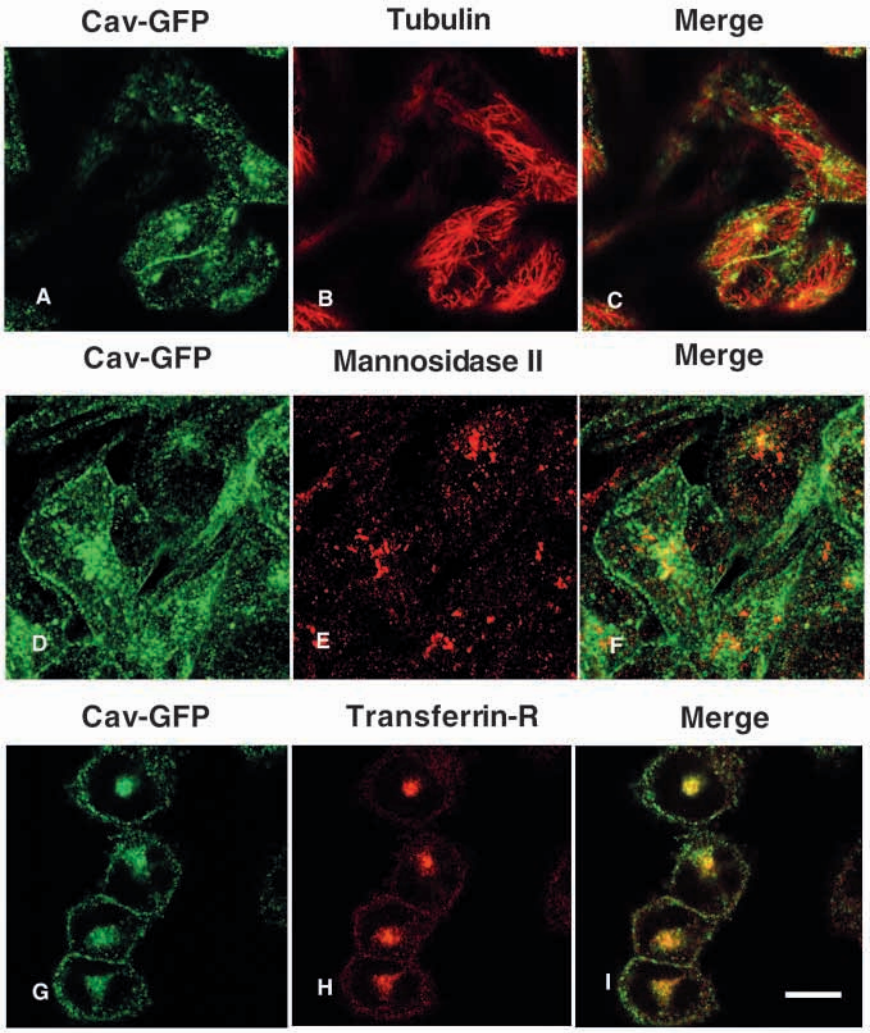

Fig. 3. Caveolin-1-GFP is localized at the MTOC, in close proximity to recycling endosomes. CHO cells stably expressing caveolin-1-GFP were plated on coverslips and processed for confocal imaging. Cells were then fixed and labeled either with anti-mannosidase II to stain the Golgi (B), anti-tubulin to stain microtubules (E) or anti-transferrin receptor antibody to stain recycling endosomes (G). Secondary antibodies were either Alexa-568-conjugated goat anti-rabbit IgG or Alexa-595-conjugated goat anti-mouse IgG. The green channel shows the distribution of caveolin-1-GFP (A,D,G) and the red channel the distribution of mannosidase II (B), tubulin (E) or the transferrin receptor (H). Merged images are shown in panels C, F and I. Each picture is a single confocal image through the center of the cell. Bar, 10 μm.

These observations suggest that caveolae can pinch off or elongate from the plasma membrane and travel into the cell, but ordinarily only a minor fraction of the total caveolae exhibit such activity during short time intervals. To determine whether the caveolin-1-GFP located in the peri-centrosomal region of the cell was exchanging with the other pools of caveolin-1-GFP we performed fluorescence recovery after photobleaching experiments (FRAP). The peri-centrosomal region of the cell was completely bleached using the 488 laser at full power for 2 seconds and recovery monitored over a 5 minute and 40 second recovery period. Fig. 5 shows images taken before bleaching, immediately after bleaching (0 time) and 5 minutes after the bleach period. Recovery was apparent within approximately 1 minute and there was a clear accumulation of GFP in the same region by 3 minutes. Quantification of the photobleached area demonstrated that recovery was 100% when the decrease in the overall signal due to FRAP-independent bleaching was subtracted. Recovery was not affected by pretreatment of the cells with cyclohexamide indicating that caveolin-1-GFP was being transported from the other regions of the cell and was not due to new synthesis. The movie of the bleach and recovery can be viewed online (Fig. 5A).

Effects of disrupting microtubules

Both the speed of caveolin-1-GFP movements within the cell and the fact that they followed curvilinear paths suggested that cavicles were traveling along microtubules. This was confirmed by treating caveolin-1-GFP expressing cells with nocodazole to depolymerize microtubules. Almost all caveolin-1-GFP movement ceased under these conditions (Fig. 6A; see also movies online). Unexpectedly, nocodazole also caused caveolin-1-GFP to accumulate on the cell surface in linear arrays that were most apparent near the bottom surface of CHO cells (Fig. 6B). The caveolin-1-GFP in the linear arrays was nearly immobile, and even the tethered movements were reduced.

The linear arrays of caveolin-1-GFP that were amplified by nocodazole were reminiscent of stress fibers, which represent bundles of actin filaments. Accordingly, we used fluorescent phalloidin to compare the distributions of actin filaments and caveolin-1-GFP. Surprisingly, linear arrays of caveolin-1-GFP were not always aligned along or adjacent to stress fibers in nocodazole-treated cells (Fig. 7) and were occasionally found in areas where fluorescent phalloidin staining was weak or absent.

We also examined the effects of nocodazole on the behavior of endogenous caveolin-1 in normal human fibroblasts (Fig. 8). A significant amount of caveolin-1 is normally organized in linear arrays in these cells (Fig. 8A); however, the number and thickness of these arrays increased markedly after cells were exposed to nocodazole (compare Fig. 8A with 8C). Anti-tubulin staining showed that the microtubules had been disrupted by the nocodazole treatment (compare Fig. 8B with 8D). A similar redistribution of endogenous caveolin-1 into linear arrays was observed in NIH3T3 cells and rat embryo fibroblasts (data not shown). When normal human fibroblasts treated with nocodazole were examined by electron microscopy, we saw a more than twofold increase in the number of invaginated caveolae (Fig. 8E). These structures were positive for immunogold labeling with anti-caveolin-1 (data not shown). This increase was quantified using numerous micrographs and the data is presented in Table 1. We conclude that microtubules are required for long-range movement of caveolin-1 positive structures and in their absence both caveolin-1 and invaginated caveolae accumulate at the cell surface.

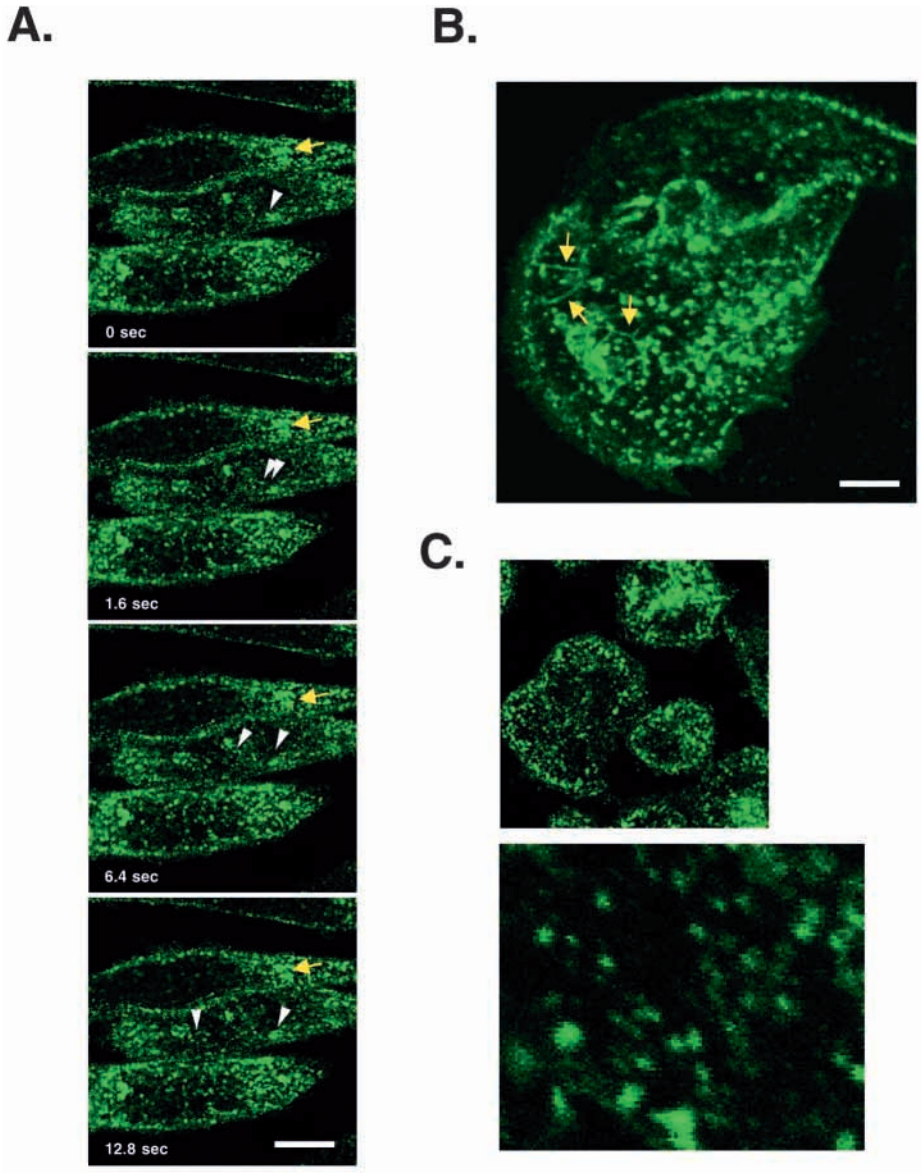

Fig. 4. Caveolin-1-GFP displays three different types of movement. Cells were plated 48 hours before use into culture dishes that had a glass coverslip glued to the bottom. Confocal sections were taken at 1.6 second intervals near the bottom of the cell, just under the nucleus in cells stably expressing caveolin-1-GFP. (A) Some of the caveolin-1-GFP in these cells showed only saltatory movements (yellow arrows). A 12.8 second recording showed, however, that other patches of caveolin-1-GFP in the same cell rapidly moved apart (follow white arrows). (B) A third population of caveolin-1-GFP was associated with dynamic tubular structures (yellow arrows), which can also be seen in the accompanying movie. (C) Stills from two videos showing examples of long range and saltatory movement in control cells. Bar, 10 μm (A); 5 μm (B). The movies that correspond to panels B and C can be viewed online (http://jcs.biologists.org/supplemental).

Effects of disrupting the actin cytoskeleton

The arrangement of caveolae in linear arrays, particularly in fibroblasts, has been described before and is believed to be due to an association of caveolae with the cortical actin cytoskeleton (Izumi et al., 1989). To determine if actin was involved in organizing the caveolin-1 into these linear arrays, we looked at the combined effects of nocodazole and drugs known to disrupt actin filaments (Fig. 9). Cells expressing caveolin-1-GFP were

incubated in the presence (Fig. 9B,D,F) or absence (Fig. 9A,C,E) of nocodazole plus either media alone (Fig. 9A,B), cytochalasin D (Fig. 9C,D), which partially disassembles actin filaments, or latrunculin A (Fig. 9E,F) which depolymerizes actin filaments completely. Projection images of the entire stack of control cells showed a patchy distribution of caveolin-1-GFP with prominent accumulations in the center of the cell (arrows). Nocodazole treatment caused the peri-centrosomal accumulations of caveolin-1-GFP to disappear with a concomitant appearance of linear arrays at the cell surface (Fig. 9B). Cytochalasin D at low concentrations had little effect on the overall distribution of caveolin-1-GFP (Fig. 9C) but completely prevented the formation of linear arrays in nocodazole treated cells (Fig. 9D). Latrunculin A, by contrast, dramatically increased the amount of caveolin-1-GFP both in the center of the cell and in irregularly shaped structures dispersed throughout the cytoplasm. This was accompanied by a loss of caveolin-1-GFP from the cell surface (Fig. 9E). In cells exposed to both latrunculin A and nocodazole (Fig. 9F), caveolin-1-GFP was only found in dispersed, irregularly shaped structures and no longer accumulated at the center of the cell. The results of these experiments indicate that cortical actin filaments confine and organize caveolae near the cell surface while microtubules carry cavicles that have been released from actin tethers into the cell.

The effects of latrunculin A on the localization of caveolin-1-GFP could be better appreciated by following the marker at early times after cells were exposed to the drug (Fig. 10A). Within 1 minute of exposure to latrunculin A, there was a massive increase in the inward movement of the caveolin-1-GFP. Aggregates of caveolin-1-GFP positive structures began to separate from the plasma membrane and migrate towards the center of the cell (Fig. 10A, 1 min; see also movies online). By 10 minutes, most cells were rounding up but remained attached to the substratum by several elongated processes. They persisted in this state for several hours. Caveolin-1-GFP could be seen moving rapidly into and out of these processes as well as throughout other regions of the cell (Fig. 10A, 10 min; see also movies online). By 20-30 minutes there was an obvious accumulation of the caveolin-1-GFP in the center of the cell and cavicles could still be seen moving towards and away from this region (Fig. 10A, 30 min). These rapid movements occurred along microtubules because they were completely eliminated when cells were treated with both nocodazole and latrunculin A (Fig. 6C; see also movies online). Live cells were

Table 1. Quantification of the nocodazole-induced increase in surface caveolae

Treatment	Number of cells	Number of caveolae	Length (cm)	Caveolae/ unit length	% increase
None	142	593	0.2	0.3	
Nocodazole	143	1102	0.15	0.73	155

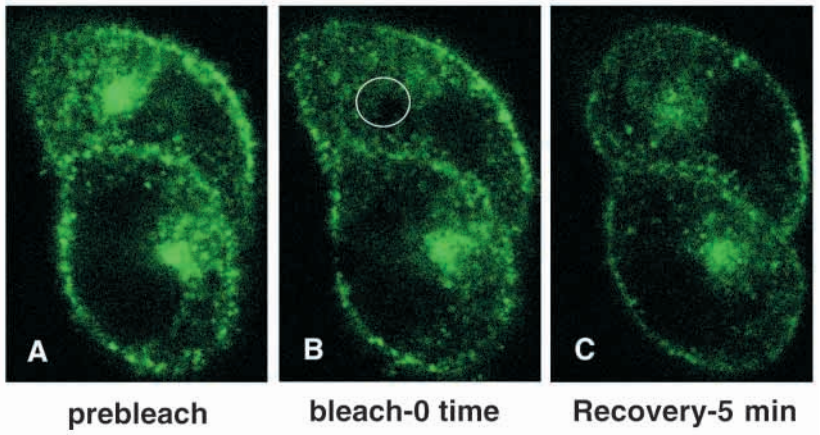

Fig. 5. FRAP analysis showing that there is active exchange between caveolin-1-GFP located in the peri-centrosomal region and the other pools of caveolin. Cells stably expressing caveolin-1-GFP were plated 48 hours before viewing into culture dishes that had a glass coverslip glued to the bottom. Confocal images were taken at 1.6 second intervals for approximately 1 minute and then the entire peri-centrosomal region of the upper cell was bleached in 6 spots for 2 seconds each using the 488 laser at full power. Immediately following the bleach, images were again collected at 1.6 second intervals for another 5 minutes and 40 seconds. Panel A shows the prebleach image and peri-centrosomal accumulations of caveolin-1-GFP in two cells. The central accumulation in the top cell was then bleached (area within the white circle, B). Panel C shows that the accumulation at the center of the cell has recovered within 5 minutes, indicating that caveolin-1-GFP travels between the various caveolin positive compartments. The corresponding movie can be viewed online (http://jcs.biologists.org/supplemental).

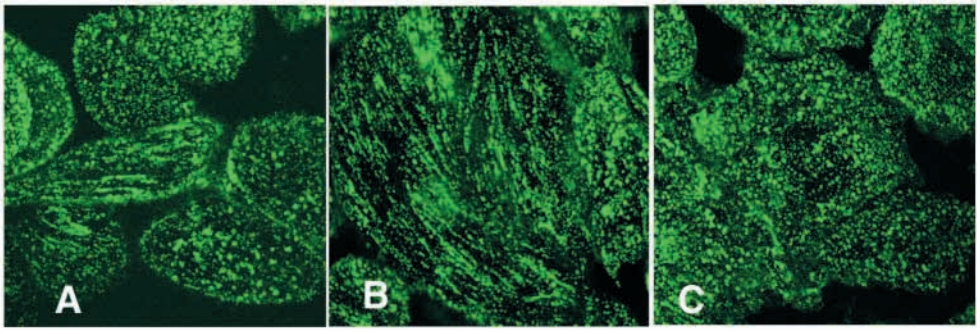

Fig. 6. Nocodazole blocks the movement of caveolin-1-GFP in live cells and organizes caveolin-1-GFP into linear arrays. CHO cells stably expressing caveolin-1-GFP were grown for 2 days before being viewed by confocal microscopy, as described in Materials and Methods. (A) Still from video of CHO cells pretreated with 10 μM nocodazole for 1 hour before viewing. Long range movements have disappeared. (B) Immunofluorescence micrograph of CHO cells pretreated with nocodazole taken at the bottom surface of the cell. (C) Still from video of stably expressing CHO cells pretreated with 10 μM nocodazole for 1 hour before the addition of 1 μM latrunculin A. Within 1 minute the arrays have disappeared and everything appears to be immobile. Bar, 10 μm. The movies that correspond to panels A and C can be viewed online (http://jcs.biologists.org/supplemental).

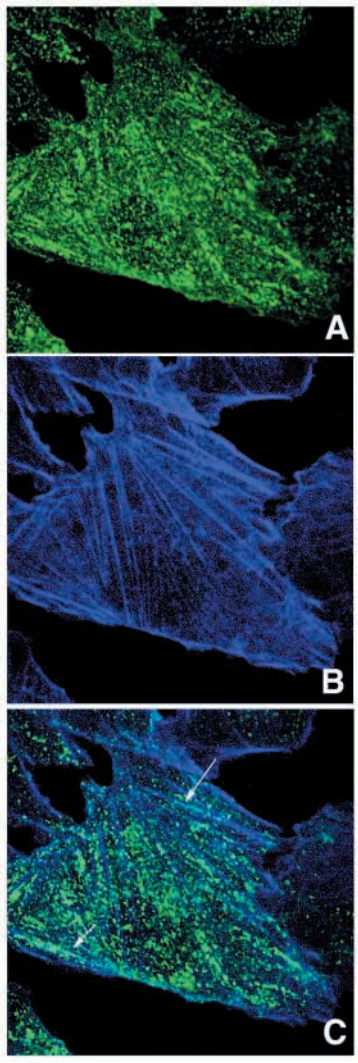

Fig. 7. Association of caveolin-1-GFP with the actin cytoskeleton. Cells stably expressing caveolin-1-GFP were plated on coverslips, grown for 2 days and treated with 10 μM nocodazole for 30 minutes before fixing with paraformaldehyde. Panel A shows the distribution of caveolin-1-GFP; panel B the distribution of F-actin stained with Alexa-633-phalloidin; and panel C a merged image. The arrows indicate regions where caveolin is aligned along or adjacent to stress fibers.

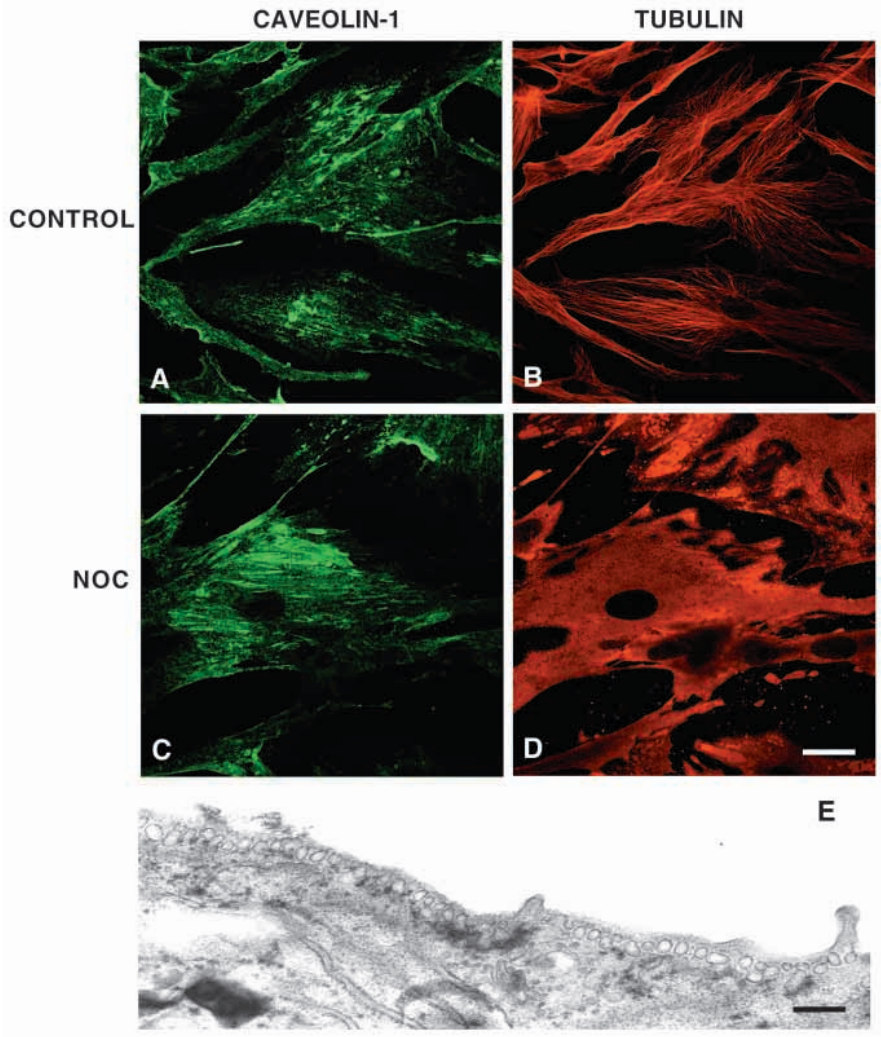

Fig. 8. Nocodazole reorganizes caveolin-1 and caveolae at the cell surface of normal human fibroblasts. (A-D) Normal human fibroblasts were grown on coverslips for 2 days. One set of cells was processed without further treatment for indirect immunofluorescence localization of caveolin-1 (A) and tubulin (B), while the other set was incubated in the presence of 40 μM nocodazole for 2 hours before staining for caveolin-1 (C) and tubulin (D). The linear arrays in the treated cells were both more extensive and thicker. (E) Normal human fibroblasts were grown in 6-well dishes for 2 days, incubated in the presence of 40 μM nocodazole for 2 hours, and processed for EM. This treatment induced a striking increase in the number of caveolae that could be detected by electron microscopy. Bars, 37 μm (A,B); 23 μm (C,D); 0.8 μm (E).

first treated for 30 minutes with nocodazole in order to form arrays and then latrunculin A was added. Within 1 minute of the addition of latrunculin A the arrays had disappeared. In the presence of both drugs there was virtually no movement. Furthermore, latrunculin A did not induce caveolin-1-GFP to accumulate near the centrosome in cells that were treated with nocodazole (Fig. 6C, Fig. 8F).

The effect of latrunculin A on the distribution of caveolin-1 in untransfected normal human fibroblasts was also examined using immunogold electron microscopy (Fig. 10B). The anti-caveolin-1 immunogold was found associated with invaginated caveolae before treatment (not shown). By contrast, within minutes after adding latrunculin A, the immunogold label was found associated with arrays of 50-70 nm invaginations that extended from the surface into the cell (e.g. between black arrows). Also common were circular profiles of membrane, containing numerous invaginated caveolae (asterisk) that appeared to have detached from the surface. A typical example of one of these clusters is shown in the inset of Fig. 10B. These structures seen by EM correspond well to the large, irregularly shaped structures that were seen by fluorescence microscopy in caveolin-1-GFP expressing cells (compare Fig. 10A and 10B). We do not know if these membrane profiles are transport intermediates or simply regions of membrane that buckled in the absence of an actin support. Nevertheless, they always contained multiple, invaginated caveolae.

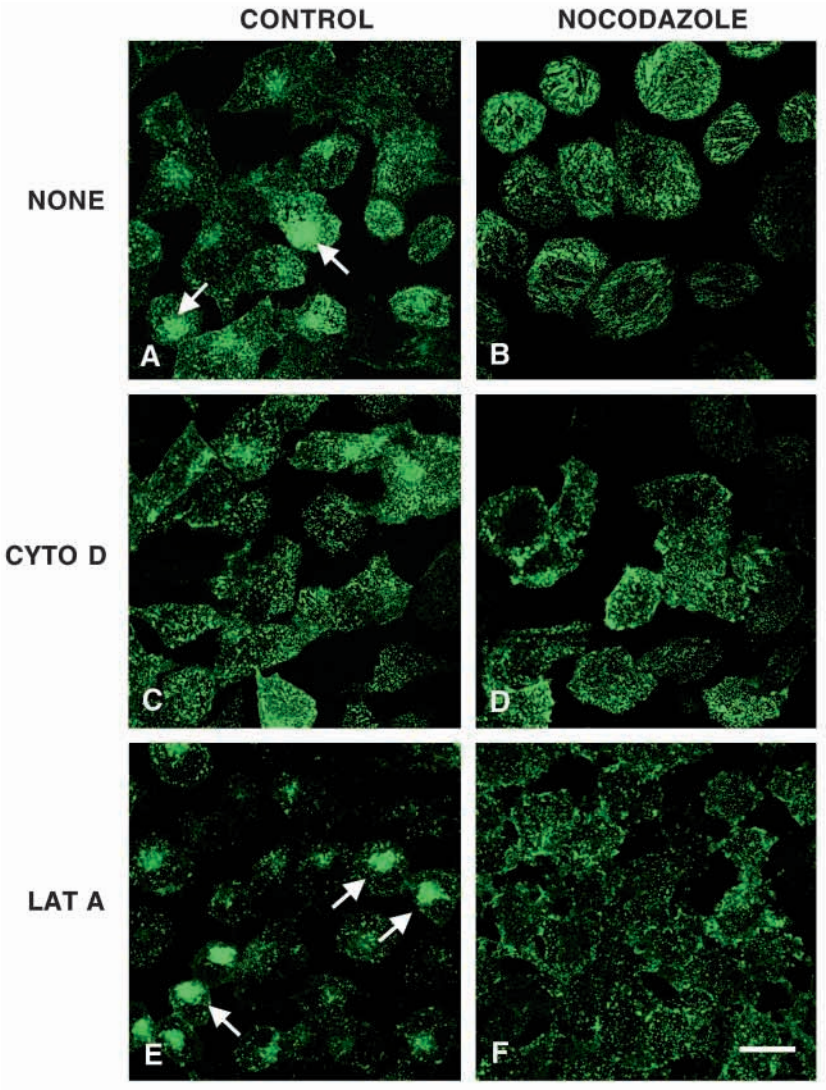

Fig. 9. Disruption of the actin cytoskeleton blocks the formation of the linear arrays of caveolin-1-GFP induced by nocodazole. CHO cells stably expressing caveolin-1-GFP were plated on coverslips and grown for 2 days, as described in Materials and Methods. Cells were incubated for 30 minutes in the absence (A,B) or presence of either 2.5 μM cytochalasin D (C,D) or 1 μM latrunculin A (E,F) and then incubated for an additional 60 minutes with (B,D,F) or without (A,C,E) 10 μM nocodazole, before fixing with paraformaldehyde and processing for visualization of GFP. Note that both cytochalasin D and latrunculin A blocked the redistribution of caveolin into linear arrays (compare B with D and F) and that nocodazole blocked the latrunculin A induced redistribution of caveolin-1-GFP to the cell center (compare E with F). Each image is the projection of a stack of confocal images that extend through the entire cell. Bar, 20 μm.

Discussion

Thanks to a few recent studies of cultured mammalian cells transiently expressing GFP-tagged versions of caveolin-1, a picture of caveolar membrane dynamics in individual cells has begun to emerge (Pelkmans et al., 2001; Thomsen et al., 2002). We have extended that approach by stably transfecting caveolin-1-GFP into a cell type, CHO, in which fluorescent caveolin-1 analogues have not been studied previously. Live cell, time-lapse microscopy of these cells revealed several novel aspects of caveolin-1 trafficking. First, we found that CHO cells, in contrast to other cell types that have been studied by similar approaches, contain an abundance of constitutively motile caveolar vesicles, or 'cavicles' that were revealed by FRAP experiments to serve as transport intermediates between plasma membrane caveolae and peri-centriolar caveosomes in the absence of specific extracellular stimuli. The finding that this form of trafficking was abolished by nocodazole indicated that microtubules serve as the tracks along which motile cavicles move. Second, the trafficking of cavicles from caveolae to caveosomes was observed to be abruptly upregulated when actin filaments were disassembled by exposure of cells to latrunculin A. The cortical network of actin filaments therefore appears to constrain either the formation of cavicles from caveolae, or the movement of newly formed cavicles towards the centrally located caveosomes. Thus, microtubules and actin filaments act coordinately to control membrane trafficking in the caveolar system. Finally, comparison of the distributions of caveosomes with other peri-nuclear endomembrane compartments emphasizes the existence of an extensive caveolar membrane system that is analogous to the endosomal membrane system and there may also be at least a partial merger of the caveosome with the recycling endosome. A model that summarizes many of these findings is presented in Fig. 11.

Recycling endosomes and the caveosomes

In CHO cells we found that caveosomes accumulated at the MTOC. This observation was reminiscent of the accumulation of caveolin containing membranes near the centrosome of A431 cells exposed to okadaic acid plus hypertonic medium (Parton et al., 1994). Not all cells accumulate caveolin-1 near the centrosome, however, because we did not observe such accumulations in human fibroblasts (data not shown). Centrosomal caveolin-1-GFP in CHO cells has a very similar distribution to that of the transferrin receptor-rich recycling endosomes (Maxfield and Yamashiro, 1987). This region of a CHO cell is difficult to resolve by immunofluorescence microscopy but careful examination of multiple stacked confocal images suggested that the two membrane systems are intertwined rather than in the same compartment. Nevertheless, the close apposition of caveosomes and recycling endosomes and their partial co-localization at the light microscope level may provide opportunities for direct communication between the caveolar and the clathrin-mediated endocytic systems.

Biochemical evidence for communication between these two membrane systems has already been reported, as anti-transferrin receptor IgG was able to immunoprecipitate both the receptor and caveolin-1 (Gagescu et al., 2000). Recycling endosomes appear to share other caveolae markers including

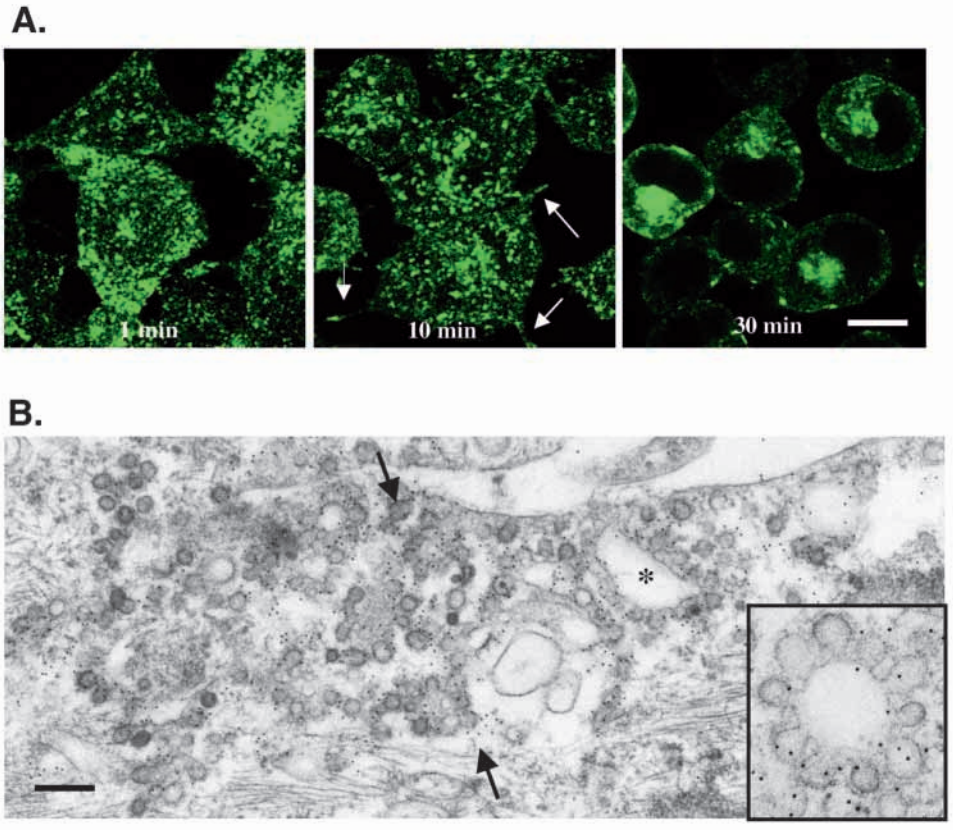

Fig. 10. Latrunculin A causes a redistribution of caveolin-1-GFP in CHO cells (A) and caveolae in normal human fibroblasts (B). (A) CHO cells stably expressing caveolin-1-GFP were treated with latrunculin A (1 μM) and the cells were imaged within 1 minute using confocal time-lapse microscopy. The three panels in A are stills from videos taken at 1.6 second intervals for a total of 6 minutes each after 1 minute, 10 minutes or 30 minutes of latrunculin A treatment. Within 1 minute there is a dramatic increase in the trafficking of caveolin-1-GFP in the cells. By 10 minutes the caveolin-1-GFP has formed larger aggregates and caveolin can be seen moving into and out of long processes that keep the cells attached to the substratum (arrows). By 30 minutes there was an accumulation of caveolin in the center of the cell. The videos taken at 1 minute and 10 minutes after latrunculin treatment can be viewed online. (B) Normal human fibroblasts were grown for 2 days and then incubated with 1 μM latrunculin A for 30 minutes before processing for immunogold localization of caveolin-1. Numerous large caveolin-positive structures were seen that appeared to have multiple invaginated caveolae all around them (*). The inset shows a higher magnification of these structures. Bars, 10 μm (A); 0.24 μm (B); 0.16 μm (inset). The corresponding movies can be viewed online (http://jcs.biologists.org/supplemental).

flotillin-1, sphingomyelin and cholesterol (Gagescu et al., 2000). Moreover, the folate receptor, a GPI anchored protein that clusters in caveolae (Ying et al., 1992), has been found in recycling endosomes containing transferrin (Mayor et al., 1998). Perhaps this ligand entered cells through caveolae before being delivered to recycling endosomes, even though many other ligands found in recycling endosomes indisputably arrive there via the coated pit-dependent pathway. In support of this idea, our own studies looking at the uptake of rhodamine-tagged transferrin suggest that at early time points transferrin and caveolin are internalized into separate vesicles but at later time points the transferrin pathway can communicate with caveolin-1 containing compartments (data not shown).

In as much as the centrosome is the principal site of internal caveolin-1-GFP positive membranes in CHO cells, we favor the idea that this compartment corresponds to the recently described caveosome (Pelkmans et al., 2001). To date the principle markers for the caveosome are caveolin, and SV-40 virus. Caveosomes accumulated SV-40 virus that had been internalized by caveolae in CV-1 cells. The caveosomes in CV-1 cells were not clustered at the centrosome, but this difference may simply reflect cell type specific variability. A recent paper by Nichols (Nichols, 2002) also describes a distinct class of caveolin-1 positive endosomes that accumulate 10K dextran, cholera toxin, GPI-GFP and SV-40 virus. We found that our cavicles also contain 10K dextran and cholera toxin (data not shown) a finding that contrasts with the reported lack of dextran uptake in SV-40-infected CV-1 cells. One possible explanation for this difference is that during infection with the virus the caveosome is somehow modified to exclude other cargo. Further work is required before this compartment can be fully defined functionally and biochemically and to determine the extent, if any, to which caveosomes communicate with recycling endosomes.

Dual control of caveolin-1-GFP traffic

Our findings indicate that actin filaments and microtubules play opposing roles in regulating the steady state distribution of caveolin-1-GFP. Whereas the cortical actin cytoskeleton appears to confine caveolin-1-GFP at the cell surface, microtubules serve as tracks for the transport of caveolin through the cytoplasm. The speed of these microtubule based movements ranged from 0.3 μm/seconds to as high as 2 μm/second, which is consistent with dynein and kinesin directed movements of organelles and vesicles along microtubules. Although the microtubule motors responsible for cavicle motility remain to be defined, one leading candidate is the recently described minus end-directed kinesin, KIFC3. This motor reportedly moves detergent resistant membranes like caveolae along microtubules (Noda et al., 2001) Depolymerization of microtubules caused a redistribution of the caveolin-1-GFP located at the centrosome to punctate structures located throughout the cell as well as an increase in the total number of invaginated caveolae at the cell surface. In

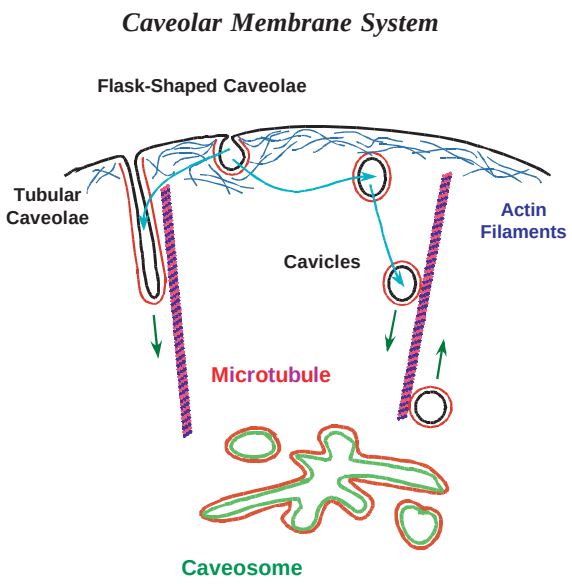

Fig. 11. A model for trafficking in the caveolar membrane system of CHO cells. Taken together, our observations suggest that cells contain a more extensive caveolar membrane system than has been previously appreciated. In CHO cells it appears to consist of a population of fairly immobile and stable caveolae at the plasma membrane, peri-centrosomal caveosomes and a population of transport intermediates that may include both cavicles and tubules that serve as bi-directional transport intermediates between caveolae and caveosomes. The cavicles move along microtubules but cortical actin filaments restrict their inward mobility. Red, caveolin-1; green, caveosome; blue, actin; pink/purple, microtubule.

contrast to the apparent trapping of caveolae at the cell surface in the absence of microtubules, elimination of actin filaments caused a marked decline in caveolin-1-GFP located near the cell surface and a corresponding increase in peri-centrosomal caveolin-1-GFP. This suggests that surface caveolae have the potential to bud from the plasma membrane and travel into the cell, but are prevented from doing so by the actin cytoskeleton.

How do actin filaments restrain the inward movement of caveolin-1? Two obvious possibilities are that cortical actin filament networks act as simple physical barriers to the detachment of caveolae from the plasma membrane or the inward movement of cavicles beyond the cortex. In either of these cases, local disassembly of cortical actin networks would be necessary to initiate inward transport of cavicles along microtubules. Another possibility is that cross-linking molecules attach caveolae or cavicles to actin filaments in the cell cortex. In this case, either removal of the cross-links or local depolymerization of actin filaments would allow cavicles to move inward. In vitro studies have shown that caveolae bud from isolated membranes in a process that requires ATP, GTP and cytosolic factors (Gilbert et al., 1999). A similar in vitro system has been used to study the budding of clathrin coated pits from purified fibroblast membrane (Lin et al., 1991). In this system release of a subpopulation of coated vesicles requires a proteolytic cleavage step to release the budding membrane from its spectrin/ankyrin linkage with the actin cytoskeleton (Kamal et al., 1998). Interestingly, only this subpopulation of vesicles is able to move along microtubules to a degradative compartment. A similar mechanism may regulate caveolae budding and cavicle traffic. Once formed from budded caveolae, cavicles may associate with motor molecules that propel them along microtubules. Actin regulation of the caveolar membrane system fits well with the growing evidence that spectrin and actin regulate membrane traffic in other membrane systems as well (Lippincott-Schwartz, 1998).

The behavior of caveolae and cavicles is highly reminiscent of the movements of pigment granules. In mammals, the pigment melanin that is deposited in the skin and hair is produced in melanocytes and transported to the cell periphery where it is secreted and then endocytosed by adjacent keratinocytes. In *dilute* mice, which lack myosin Va, the amount of secreted pigment is drastically reduced resulting in their characteristic light coat color (Wu et al., 1998). Time lapse video microscopy of wild type and *dilute* melanocytes has shown that fast, bi-directional, microtubule dependent transport of melanosomes is the mechanism responsible for long range transport of melanosomes, while accumulation at the dendritic tips where they are secreted is due to the myosin Va dependent capture of these organelles in the actin-rich periphery. This generates an actin-filament dependent polarized distribution of organelles that are transported bi-directionally along microtubules. Several unconventional myosins have now been implicated in organelle transport (reviewed by Tuxworth and Titus, 2000). These include a related, myosin V dependent mechanism that regulates pigment granule distributions in fish scale melanophore cells (Rodionov et al., 1998; Rogers and Gelfand, 1998), the involvement of myosin1α in the movement and distribution of lysosomes (Cordonnier et al., 2001), and a role for myosin VI in clathrin mediated endocytosis (Buss et al., 2001). It will be interesting to learn whether any myosins are similarly involved in establishing the steady state enrichment of caveolae at the plasma membrane, and of caveosomes near the centrosome.

Our data are in strong agreement with the results obtained by other investigators who have used caveolin-GFP (Pelkmans et al., 2001) or GFP-caveolin (Thomsen et al., 2002) to demonstrate that cell surface caveolae are relatively stationary. They are also consistent with a report that GFP-caveolin-1 is present on a population of relatively motile structures scattered throughout the cytoplasm (Thomsen et al., 2002). In other respects, however, our results seem to be at odds with those reported in prior similar studies. For example, caveolin-1-GFP was used to demonstrate that binding of SV-40 virus could trigger internalization of caveolar membranes from the surface of CV-1 cells, which was rarely observed in the absence of virus (Pelkmans et al., 2001). Although SV-40 can clearly induce uptake of caveolae, it is not clear what normally initiates this process in virus-free cells. Our data indicate that in CHO cells, at least, caveolae are internalized constitutively, albeit at lower rates than have been observed for clathrin coated pit uptake. Likewise, photobleaching of peri-centrosomal GFP-caveolin-1 in transiently transfected HeLa cells (Thomsen et al., 2002) was followed by fluorescence recovery that was much slower than we observed in CHO cells that stably expressed caveolin-1-GFP. Although the causes of this discrepancy are unknown, leading suspects include cell type-specific differences in caveolar membrane trafficking, functional differences between GFP-caveolin-1 and caveolin-1-GFP, and overexpression of GFP-caveolin-1 in the

transiently transfected HeLa cells. The last possibility seems especially likely, because the low level of FRAP that was observed in HeLa cells whose peri-centrosomal regions were photobleached was abolished by pretreating the cells with cycloheximide. This implies that GFP-caveolin-1 was accumulating in the Golgi complex of the HeLa cells as a result of overexpression. In contrast, we show here that caveolin-1-GFP in stably transfected CHO cells was expressed at low levels relative to endogenous caveolin-1, and that peri-centrosomal caveolin-1-GFP in the CHO cells was not associated with the Golgi, but rather with caveosomes that fortuitously accumulated near the MTOC. This allowed us to bleach caveosomes selectively and to show that rapid trafficking of caveolin-1-GFP to these organelles occurred continuously in the presence of cycloheximide. In CV-1 cells Pelkmans et al. (Pelkmans et al., 2001) also only saw caveolin-1-GFP in the Golgi apparatus in a few cells that were highly overexpressing the fusion protein. More work is needed to determine if these are cell-specific differences in caveolar membrane traffic, or simply reflect the influence of the probes used to monitor the movement of these membranes. Whatever the explanation proves to be, the caveolar membrane system is clearly more extensive and dynamic than has been previously appreciated.

We thank Brenda Pallares for administrative assistance and Peter Michaely for critical reading of the manuscript. This work was supported by grants from the National Institutes of Health, HL 20948, GM 52016, DK 52395 and the Perot Family Foundation.

References

Al-Haddad, A., Shonn, M. A., Redlich, B., Blocker, A., Burkhardt, J. K., Yu, H., Hammer, J. A., 3rd, Weiss, D. G., Steffen, W., Griffiths, G. et al. (2001). Myosin Va bound to phagosomes binds to F-actin and delays microtubule-dependent motility. *Mol. Biol. Cell* **12**, 2742-2755.

Anderson, R. G. (1998). The caveolae membrane system. *Annu. Rev. Biochem.* **67**, 199-225.

Anderson, R. G., Kamen, B. A., Rothberg, K. G. and Lacey, S. W. (1992). Potocytosis: sequestration and transport of small molecules by caveolae. *Science* **255**, 410-411.

Apodaca, G. (2001). Endocytic traffic in polarized epithelial cells: role of the actin and microtubule cytoskeleton. *Traffic* **2**, 149-159.

Bloom, G. S. and Goldstein, L. S. (1998). Cruising along microtubule highways: how membranes move through the secretory pathway. *J. Cell Biol.* **140**, 1277-1280.

Brewer, C. B. (1994). Cytomegalovirus plasmid vectors for permanent lines of polarized epithelial cells. *Methods Cell Biol.* **43**, 233-245.

Bridgman, P. C. (1999). Myosin Va movements in normal and dilute-lethal axons provide support for a dual filament motor complex. *J. Cell Biol.* **146**, 1045-1060.

Buss, F., Arden, S. D., Lindsay, M., Luzio, J. P. and Kendrick-Jones, J. (2001). Myosin VI isoform localized to clathrin-coated vesicles with a role in clathrin-mediated endocytosis. *EMBO J.* **20**, 3676-3684.

Cordonnier, M. N., Dauzonne, D., Louvard, D. and Coudrier, E. (2001). Actin filaments and myosin I alpha cooperate with microtubules for the movement of lysosomes. *Mol. Biol. Cell* **12**, 4013-4029.

Dietzen, D. J., Hastings, W. R. and Lublin, D. M. (1995). Caveolin is palmitoylated on multiple cysteine residues. Palmitoylation is not necessary for localization of caveolin to caveolae. *J. Biol. Chem.* **270**, 6838-6842.

Fath, K. R. and Burgess, D. R. (1993). Golgi-derived vesicles from developing epithelial cells bind actin filaments and possess myosin-I as a cytoplasmically oriented peripheral membrane protein. *J. Cell Biol.* **120**, 117-127.

Gagescu, R., Demaurex, N., Parton, R. G., Hunziker, W., Huber, L. A. and Gruenberg, J. (2000). The recycling endosome of Madin-Darby canine kidney cells is a mildly acidic compartment rich in raft components. *Mol. Biol. Cell* **11**, 2775-2791.

Gilbert, A., Paccaud, J. P., Foti, M., Porcheron, G., Balz, J. and Carpentier, J. L. (1999). Direct demonstration of the endocytic function of caveolae by a cell- free assay. *J. Cell Sci.* **112**, 1101-1110.

Goldstein, J. L., Basu, S. K. and Brown, M. S. (1983). Receptor-mediated endocytosis of low-density lipoprotein in cultured cells. *Methods Enzymol.* **98**, 241-260.

Izumi, T., Shibata, Y. and Yamamoto, T. (1989). The cytoplasmic surface structures of uncoated vesicles in various tissues of rat as revealed by quick-freeze, deep-etching replicas. *J. Electron Microsc.* **38**, 47-53.

Kamal, A., Ying, Y. and Anderson, R. G. (1998). Annexin VI-mediated loss of spectrin during coated pit budding is coupled to delivery of LDL to lysosomes. *J. Cell Biol.* **142**, 937-947.

Kogo, H. and Fujimoto, T. (2000). Concentration of caveolin-1 in the cleavage furrow as revealed by time- lapse analysis. *Biochem. Biophys. Res. Commun.* **268**, 82-87.

Kuznetsov, S. A., Langford, G. M. and Weiss, D. G. (1992). Actin-dependent organelle movement in squid axoplasm. *Nature* **356**, 722-725.

Laemmli, U. K. (1970). Cleavage of structural proteins during the assembly of the head of bacteriophage T4. *Nature* **227**, 680-685.

Lamaze, C., Fujimoto, L. M., Yin, H. L. and Schmid, S. L. (1997). The actin cytoskeleton is required for receptor-mediated endocytosis in mammalian cells. *J. Biol. Chem.* **272**, 20332-20335.

Lin, H. C., Moore, M. S., Sanan, D. A. and Anderson, R. G. (1991). Reconstitution of clathrin-coated pit budding from plasma membranes. *J. Cell Biol.* **114**, 881-891.

Lippincott-Schwartz, J. (1998). Cytoskeletal proteins and Golgi dynamics. *Curr. Opin. Cell Biol.* **10**, 52-59.

Liu, P. and Anderson, R. G. (1995). Compartmentalized production of ceramide at the cell surface. *J. Biol. Chem.* **270**, 27179-27185.

Machleidt, T., Li, W. P., Liu, P. and Anderson, R. G. (2000). Multiple domains in caveolin-1 control its intracellular traffic. *J. Cell Biol.* **148**, 17-28.

Maxfield, F. R. and Yamashiro, D. J. (1987). Endosome acidification and the pathways of receptor-mediated endocytosis. *Adv. Exp. Med. Biol.* **225**, 189-198.

Mayor, S., Sabharanjak, S. and Maxfield, F. R. (1998). Cholesterol-dependent retention of GPI-anchored proteins in endosomes. *EMBO J.* **17**, 4626-4638.

Monier, S., Dietzen, D. J., Hastings, W. R., Lublin, D. M. and Kurzchalia, T. V. (1996). Oligomerization of VIP21-caveolin in vitro is stabilized by long chain fatty acylation or cholesterol. *FEBS Lett* **388**, 143-149.

Morris, R. L. and Hollenbeck, P. J. (1995). Axonal transport of mitochondria along microtubules and F-actin in living vertebrate neurons. *J. Cell Biol.* **131**, 1315-1326.

Nichols, B. J. (2002). A distinct class of endosome mediates clathrin-independent endocytosis to the Golgi complex. *Nat. Cell Biol.* **4**, 374-378.

Noda, Y., Okada, Y., Saito, N., Setou, M., Xu, Y., Zhang, Z. and Hirokawa, N. (2001). KIFC3, a microtubule minus end-directed motor for the apical transport of annexin XIIIb-associated Triton-insoluble membranes. *J. Cell Biol.* **155**, 77-88.

Palade, G. E. (1953). Fine Structure of Blood Capillaries. *J. Appl. Phys.* **24**, 1424.

Parton, R. G., Joggerst, B. and Simons, K. (1994). Regulated internalization of caveolae. *J. Cell Biol.* **127**, 1199-1215.

Pelkmans, L., Kartenbeck, J. and Helenius, A. (2001). Caveolar endocytosis of simian virus 40 reveals a new two-step vesicular-transport pathway to the ER. *Nat. Cell Biol.* **3**, 473-483.

Rodionov, V. I., Hope, A. J., Svitkina, T. M. and Borisy, G. G. (1998). Functional coordination of microtubule-based and actin-based motility in melanophores. *Curr. Biol.* **8**, 165-168.

Rogers, S. L. and Gelfand, V. I. (1998). Myosin cooperates with microtubule motors during organelle transport in melanophores. *Curr. Biol.* **8**, 161-164.

Rogers, S. L. and Gelfand, V. I. (2000). Membrane trafficking, organelle transport and the cytoskeleton. *Curr. Opin. Cell Biol.* **12**, 57-62.

Rothberg, K. G., Heuser, J. E., Donzell, W. C., Ying, Y. S., Glenney, J. R. and Anderson, R. G. (1992). Caveolin, a protein component of caveolae membrane coats. *Cell* **68**, 673-682.

Simionescu, N. (1983). Cellular aspects of transcapillary exchange. *Physiol. Rev.* **63**, 1536-1579.

Smart, E. J., Ying, Y. S., Conrad, P. A. and Anderson, R. G. (1994). Caveolin moves from caveolae to the Golgi apparatus in response to cholesterol oxidation. *J. Cell Biol.* **127**, 1185-1197.

Thomsen, P., Roepstorff, K., Stahlhut, M. and van Deurs, B. (2002).

Caveolae are highly immobile plasma membrane microdomains, which are not involved in constitutive endocytic trafficking. *Mol. Biol. Cell* **13**, 238-250.

Tuxworth, R. I. and Titus, M. A. (2000). Unconventional myosins: anchors in the membrane traffic relay. *Traffic* **1**, 11-8.

Valetti, C., Wetzel, D. M., Schrader, M., Hasbani, M. J., Gill, S. R., Kreis, T. E. and Schroer, T. A. (1999). Role of dynactin in endocytic traffic: effects of dynamitin overexpression and colocalization with CLIP-170. *Mol. Biol. Cell* **10**, 4107-4120.

Volonte, D., Galbiati, F. and Lisanti, M. P. (1999). Visualization of caveolin-1, a caveolar marker protein, in living cells using green fluorescent protein (GFP) chimeras. The subcellular distribution of caveolin-1 is modulated by cell-cell contact. *FEBS Lett.* **445**, 431-439.

Wu, X., Bowers, B., Rao, K., Wei, Q. and Hammer, J. A. (1998). Visualization of melanosome dynamics within wild-type and dilute melanocytes suggests a paradigm for myosin V function in vivo. *J. Cell Biol.* **143**, 1899-1918.

Yamada, E. (1955). The fine structure of the gall bladder epithelium of the mouse. *J. Biophys. Biochem. Cytol.* **1**, 445-458.

Ying, Y. S., Anderson, R. G. and Rothberg, K. G. (1992). Each caveola contains multiple glycosyl-phosphatidylinositol-anchored membrane proteins. *Cold Spring Harbor Symp. Quant. Biol.* **57**, 593-604.